Pramāṇa – J. Phys., Vol. 33, No. 4, October 1989, pp. 481–492. © Printed in India.

A new representation of the heavy ion Coulomb potential

P BASU, P BHATTACHARYA and M L CHATTERJEE
Saha Institute of Nuclear Physics, 1/AF, Bidhannagar, Calcutta 700064, India

MS received 17 October 1988; revised 15 March 1989

Abstract. The Coulomb potential between two heavy ions at their interpretation condition has been represented in terms of two point charges with reduced effective charge, dependent on overlap volume. This representation enables visualization of the dynamic development of the deformations of the colliding nuclei as a function of the degree of overlap. The potential has been compared with well known potentials for heavy-ion collisions. This Coulomb potential gave good agreement in reproducing excitation functions for fusion for a large number of heavy-ion systems.

Keywords. Coulomb potential; heavy ions; overlap volume; deformation.

PACS No. 25·70

1. Introduction

In all types of two-body interactions between heavy ions, be it fission, fusion or scattering, the mutual Coulomb potential plays an important role (Bondorf *et al* 1974; Birkelund *et al* 1979). The potential will necessarily maintain the D^{-1} dependence at large distances. But the main difficulty arises for distances of separation D, smaller than the touching sphere configuratin (vide figure 1). It is well known that for fusion to occur, the Coulomb energy-changes in the regions of smaller distances of separation ($D < R_H + R_L$) must be markedly off from the D^{-1} potential. The ion-ion potential, used in optical model calculations (point charge within a sphere approximation), as well as the Bondorf potential (Bondorf *et al* 1974; Birkelund *et al* 1979) are used extensively to generate a negative hump (well) for sustaining fusion states. Both these

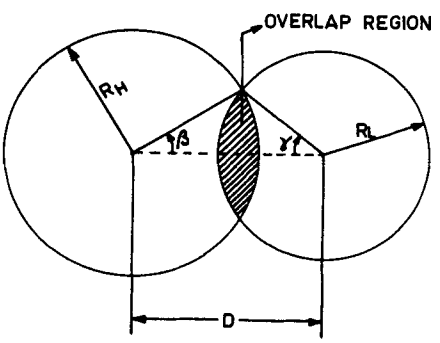

Figure 1. Schematic view of two heavy ions interpenetrating each other. The shaded region shows the overlap. D is the distance of separation between the two centres.

potentials adopt a slower variation for distances smaller and away from the touching sphere configuration.

The Bondorf potential retains the D^{-1} form at large distances ($D \geqslant R_H + R_L$), and for smaller distances has the form

$$V_B(D) = V_0 - kD^n, \quad D < R_C \quad (R_C = R_H + R_L) \tag{1}$$

where R_H and R_L are the radii of impinging heavy and light ions, respectively. Here V_0 (the Bondorf potential at $D = 0$) is so chosen, that it essentially represents the difference between the self Coulomb energies of the heavy and light nuclei as a composite system and their separate entities:

$$V_0 = (3/5)e^2\left[\frac{(Z_H + Z_L)^2}{(R_H^3 + R_L^3)^{1/3}} - \frac{Z_H^2}{R_H} - \frac{Z_L^2}{R_L}\right] \tag{2}$$

n and k are two separate parameters. Though this form is simple, the actual calculation of n and k requires involved parametrizations. Moreover it is not possible to get any insight into the physical picture of the region $D < (R_H + R_L)$. The ion-ion potential for distances $D < R_C$ is given by

$$V_I(D) = \frac{Z_H Z_L e^2}{2R_C}\left[3 - \frac{D^2}{R_C^2}\right] \tag{3}$$

where $R_C = R_H + R_L = r_0(A_H^{1/3} + A_L^{1/3})$.

Another potential was tried (Wilczynski and Siwek-Wilczynska 1975) where predominantly a D^{-1} potential was used excepting at extremely small values of D, in which the blow-up of the potential at $D = 0$ was avoided by a suitable choice of the denominator.

For all these potentials in the region of $D < R_C$, the dependence on D differs considerably from the D^{-1} dependence at larger radial separation. In our approach when the two ions interpenetrate each other, i.e. for $D < R_C$, we still preserve the D^{-1} form of the potential, replacing the charges Z_H and Z_L of the heavy and light ions, by their effective values, which are functions of the degree of interpretation, or the overlap volume. It is only at very small distances ($D \simeq 0$) that the denominator is chosen in analogy with that of Wilczynski *et al* (Wilczynski and Siwek-Wilczynska 1975), such that a finite value of the Coulomb potential at the origin, may be obtained.

Mention should also be made of realistic calculation of electrostatic potentials between the two heavy ions, considered as two Fermi charge distributions (Jain *et al* 1975). These realistic calculations always lead to an overestimation of the Coulomb potential for distances $D < R_C$, and as a result are seldom used for heavy-ion fusion calculations. A degree of the overestimation of these types of calculations can be gauged from a comparison of different models given (Birkelund *et al* 1979). Moreover, no account of volume conservation is taken into consideration in these calculations. The heavy ion Coulomb potentials have been extensively reviewed by Hodgson in a text book (Hodgson 1978).

2. Formalism of the model

In our prescription we have $Z_H \cdot Z_L \cdot e^2/D$ (i.e. D^{-1} potential) as the Coulomb potential for $D \geqslant R_H + R_L$. At distances $D < R_H + R_L$ the two ions interpenetrate each other, (figure 1) we use the $1/(D + \delta)$ form similar to that of Wilczynski and Siwek-Wilczynska

1975). However the charges of the respective partners viz. Z_H and Z_L are replaced by their effective values, which are functions of the overlap volume. The shaded portion in figure 1 shows the overlap region. The overlap volume Ω derived from geometrical consideration and integration of the volume elements in the shaded region is given by

$$\Omega = \frac{\pi R_H^3}{3}(2 - 3\cos\beta + \cos^3\beta) + \frac{\pi R_L^3}{3}(2 - 3\cos\gamma + \cos^3\gamma) \tag{4}$$

where the angles β and γ are functions of the distance of separation D.

$$\cos\beta = (D^2 + R_H^2 - R_L^2)/2R_H D, \quad \cos\gamma = (D^2 - R_H^2 + R_L^2)/2R_L D.$$

We also define the degree of overlap as Ω/V_L, where $V_L = 4/3\pi R_L^3$ = volume of the lighter partner, and $R_{H(L)} = r_0 A_{H(L)}^{1/3}$, where $r_0 = 1{\cdot}16$ for Bondorf and our form of potential, and $r_0 = 1{\cdot}3$ for ion-ion potential.

The overlap volume (Ω) increases with increasing interpenetration between the two ions. Due to this physical overlap the charge and nucleonic distribution changes depending upon the degree of overlap. Such rearrangement of nucleonic distribution and the flow of matter in transverse direction (path of minimum resistance) has been suggested in heavy ion collisions (Scheid *et al* 1968). In invoking the idea of molecular configurations in heavy ion collisions (Park *et al* 1981) used an imaginary potential in the optical model whose strength is proportional to the overlap volume between the two nuclei. Thus understanding of heavy ion collisions in the region of smaller separation (i.e. larger overlap volume) in terms of overlap volume is a macroscopic picture, in complete conformity with the two centered shell model picture (Maruhn and Greiner 1972; Fink *et al* 1974). At large distances of separation there are two separate nuclei with distinct potential wells and single-particle (s.p.) states, with minimum mutual interactions (excepting Coulomb). At very small separations the two potential wells overlap and ultimately merge into a single potential and accompanying s.p. states correspond to complete fusion. In the intermediate region the interaction or absorption potential is determined by the degree of overlap.

For collisions viewed macroscopically at such distances the nucleons in the overlap volume are under the influence of strong interactions as a result, a) the two surfaces in the zone of interpenetration disappear and a deformed surface evolves; b) under the assumption of nuclear incompressibility (particularly for low energy collisions), the density doubling in the overlap zone is not permissible and as a result the nucleons flow out forming a transverse bulge (Birkelund *et al* 1979; Scheid *et al* 1968). Clearly we see that nuclei do not behave as frozen spheres. The nuclei deform and the dynamical shapes at smaller separation (D) differ very much from the configurations of two spheres in contact or further away. The excess nucleons within the overlap volume (under the normal density constraint) phase out of the dinuclear interface and this might play a significant role in the formation of neck in fission or fusion processes.

As mentioned earlier we shall retain an approximate D^{-1} form, and to match the fusion requirements we propose a decrease of the effective charge of the two spheres as a function of the overlap volume. The functional form is as follows:

$$Z_H(\text{eff}) = Z_H\left(1 - K(\Omega)\frac{\Omega}{V_H}\right); \quad Z_L(\text{eff}) = Z_L\left(1 - K(\Omega)\frac{\Omega}{V_L}\right) \tag{5}$$

where V_H and V_L are the volumes of the heavy and light partners respectively. K is a slowly varying function of the overlap volume (Ω). The effective charge expression actually means that a certain fraction $K(\Omega)$ of the charge contained in the overlap zone do not effectively contribute to the mutual Coulomb repulsion because of rearrangement or flow out of nuclear matter. Thereby we still retain an approximate point charge hypothesis, but with a reduced total charge for each of the colliding systems so long as the overlap persists. But for distances $D \geqslant (R_H + R_L)$, the overlap vanishes and the colliding spheres mutually repel with the full charge.

The form of the Coulomb potential proposed is as follows:

$$V_C(D) = \frac{Z_H(\text{eff})Z_L(\text{eff})e^2}{D+\delta} \tag{6}$$

where

$$\delta = \chi e^{-D/A}$$

$$\chi = 0{\cdot}09(A_H + A_L)^{1/3}$$

$$A = \text{Range parameter} = 0{\cdot}1(R_H - R_L) + 1, \text{in fm}.$$

The exponential form of δ ensures that the potential speedily attains D^{-1} form at higher values of D. The expression for χ shows its dependence on the size of the total system. The range parameter A has small dependence on the asymmetry between the colliding partners and its value is 1 fm for symmetric systems.

By trial it was found that the following functional form of $K(\Omega)$ worked well for a very wide range of asymmetries including all symmetric and near symmetric systems.

$$K(\Omega) = \frac{0{\cdot}182\left[3 - 1{\cdot}5\left(\dfrac{A_H - A_L}{A_H + A_L}\right)^2\right]}{1 - \left(\dfrac{\Omega}{V_H + V_L}\right)^2} \tag{7}$$

For symmetric systems

$$K(\Omega) = \frac{0{\cdot}546}{1 - \frac{1}{4}(\Omega/V_L)^2}, \quad \text{where } A_H = A_L,\ V_H = V_L.$$

3. Results

We have computed this potential over a wide range of D, for various combinations of colliding nuclei from ^{12}C to ^{208}Pb, as shown in figure 2. The overall agreement for all such systems with Bondorf potential (Bondorf *et al* 1974) is within 5–6%, over the large range of overlap (up to 60%) defined by Ω/V_L ratios, as indicated in the upper scales of figure 2. Variations of K for different systems are shown in figure 3.

It may be mentioned that the polarization dependent potential is at the most 1% of the normal static potential (Broglia and Winther 1981; Bohr and Mottelson 1975; Banerjee *et al* 1985) for the region of overlap considered here. We do not claim accuracy of more than a few per cent and hence it is not considered here.

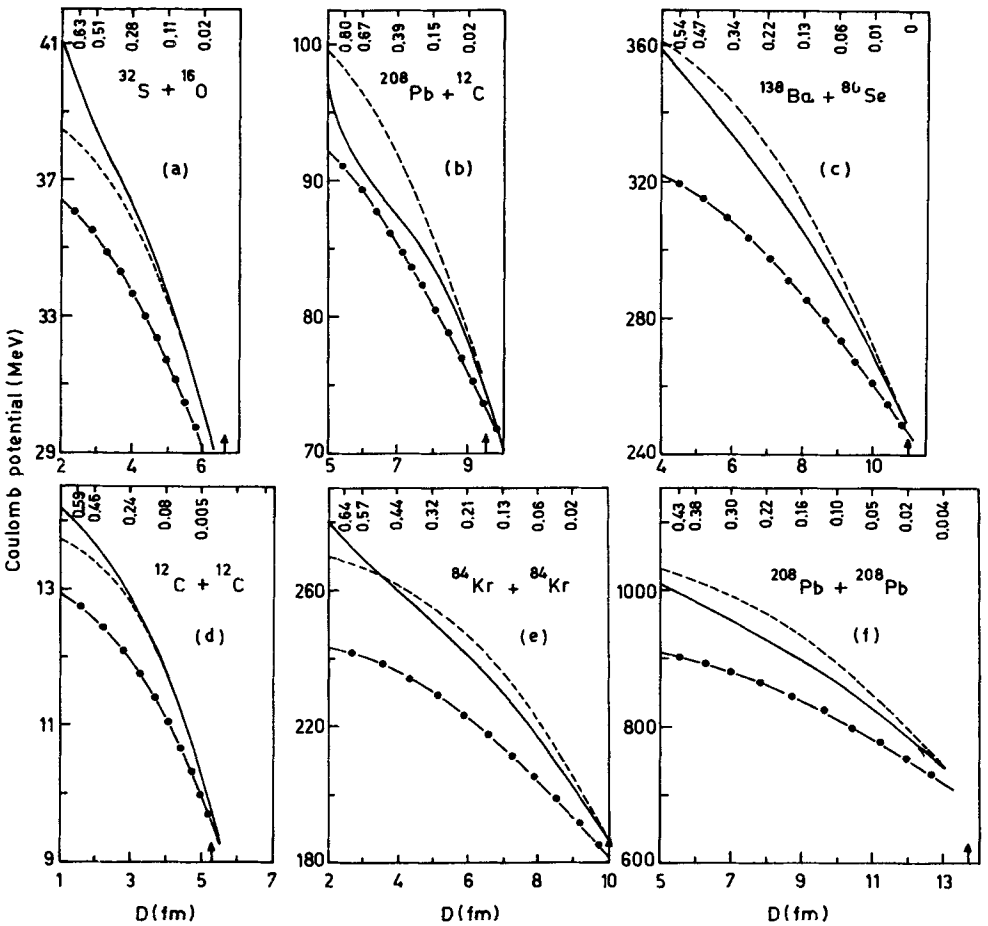

Figure 2. Coulomb potentials for different heavy ion systems plotted against D. ———— Present model ($r_0 = 1{\cdot}16$), — — — Bondorf potential ($r_0 = 1{\cdot}16$), —●—●—●— Ion-ion potential ($r_0 = 1{\cdot}3$). Upper horizontal scale gives the degree of overlap (Ω/V_L ratio). The vertical arrow in the D-axis designates the touching sphere configuration (i.e. $D = R_H + R_L$).

4. Heavy-ion fusion

We have applied our effective Coulomb formalism to calculate heavy-ion fusion excitation functions, over a wide range of mass and energy. Fusion excitation functions depend combinatively on (a) the Coulomb potential, (b) the nuclear ion-ion potential, and (c) the dissipative forces. For (b) we have used the standard nuclear proximity potential (Blocki *et al* 1977), and for (c), the one-body proximity function (Randrup 1978). This model is developed to the same degree of accuracy as the conservative nuclear force by virtue of the proximity treatment.

Having defined $V_N(D)$, $V_C(D)$ and the dissipative forces, we next solve the classical equations of motion. The four dynamical variables used in this calculation are D, θ,

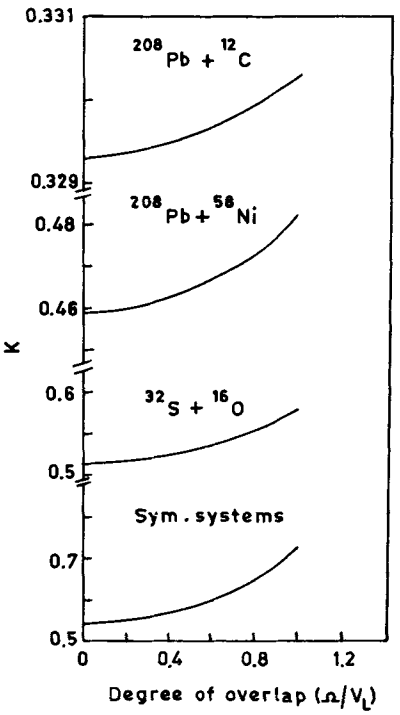

Figure 3. Variations of K against degree of overlap (Ω/V_L) for both symmetric and asymmetric systems.

θ_T and θ_P (Bondorf *et al* 1974; Birkelund *et al* 1979). From the above calculations, one determines l_f, the maximum angular momentum that fuses. In the sharp cut-off approximation the fusion cross-section σ_{fus} is given by

$$\sigma_{\text{fus}} = \pi\lambda^2 \sum^{l_f} (2l + 1). \tag{8}$$

We have used our effective Coulomb formalism to calculate fusion excitation functions for a large number of target projectile pairs, differing widely in mass and charge. Some representative results are shown in figures 4 and 5. In figure 4 data for $^{16}O + {}^{16}O$ are taken from (Weidinger *et al* 1976; Fernandez *et al* 1978; Kolata *et al* 1977; Conjeaud *et al* 1976; Tserruya *et al* 1978), $^{16}O + {}^{24}Mg$ (Tabor *et al* 1978), $^{16}O + {}^{28}Si$ (Dauk *et al* 1975; Rascher *et al* 1979), $^{35}Cl + {}^{56}Fe$ (Scobel *et al* 1976). In figure 5 data for $^{24}Mg + {}^{32}S$ are taken from (Gutbrod *et al* 1973; Kovar *et al* 1977), $^{40}Ar + {}^{109}Ag$ (Britt *et al* 1976), $^{16}O + {}^{27}Al$ (Eisen *et al* 1977; Back *et al* 1977; Kozub *et al* 1975). Fusion calculations with Bondorf Coulomb potential is also shown for comparison. It is seen that for lower energies the results for both these potentials are the same. This is in agreement with the thinking that at low energies the fusion cross-sections are model independent. At high energies, there are some deviations from the Bondorf potential, and our form of potential always predicts a larger cross-section. In fact it can be seen from the figures, that for some of the cases our potential gives better agreement with experimental observations.

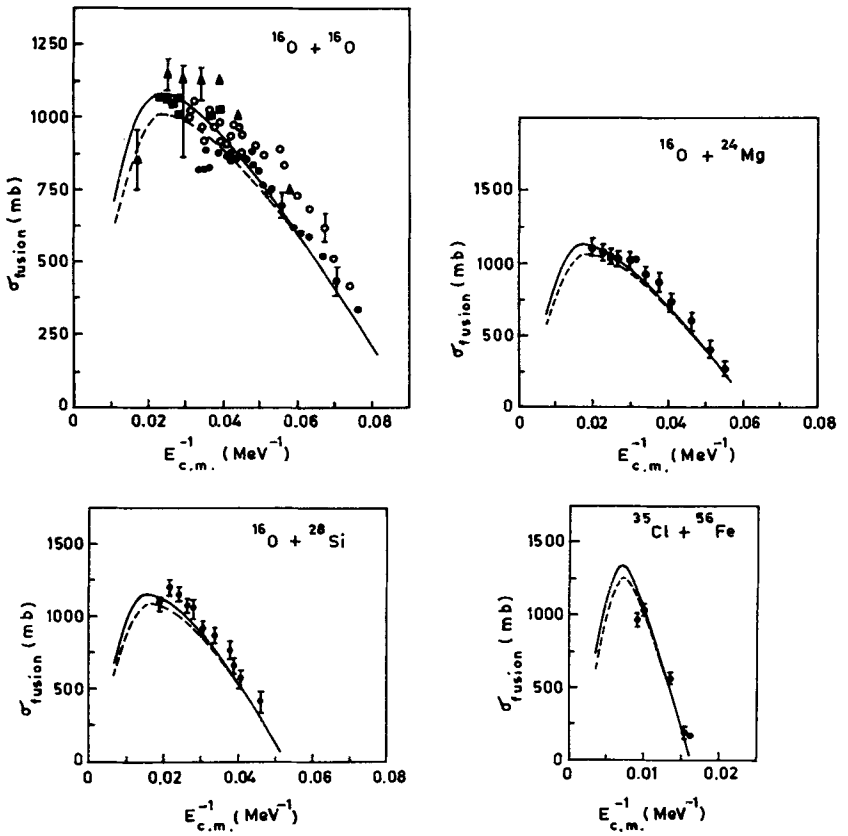

Figure 4. Fusion cross-section σ_{fus} plotted versus E_{cm}^{-1}. The solid line indicates our form of potential, while the dashed line denotes the Bondorf potential. Data for different target projectile pairs are taken from various references detailed in the text.

The fusion barrier radius R_B and barrier height V_B, for $l = 0$, are calculated and shown in table 1. Values of R_B and V_B are determined from the slope and intercept of a plot of $\sigma_{fus}(E)$ versus $1/E$. Though it may lead to sizeable ambiguity in the determination of R_B, but as a first approximation it is okay. Energy E_{cm}^M and cross-section σ_{fus}^M for the excitation fusion maximum are also shown in table 1.

The corresponding angular momentum at the maximum of excitation functions $l_f(\sigma_{fus}^M)$ are also tabulated. Table 1 also contains the respective results obtained with Bondorf potential. Here also we see satisfactory agreement with our form of Coulomb potential.

The same parametrization of the Coulomb potential has been used, for a wide range of target projectile pairs. We have seen that fusion calculations are very sensitive to r_0 values. By changing r_0, from system to system, much better agreement can be achieved. But to emphasize the generality of the potential used in widely different charge and mass regimes of the colliding ions, we have strictly stuck to a particular value of $r_0 (= 1{\cdot}16)$, in all these calculations.

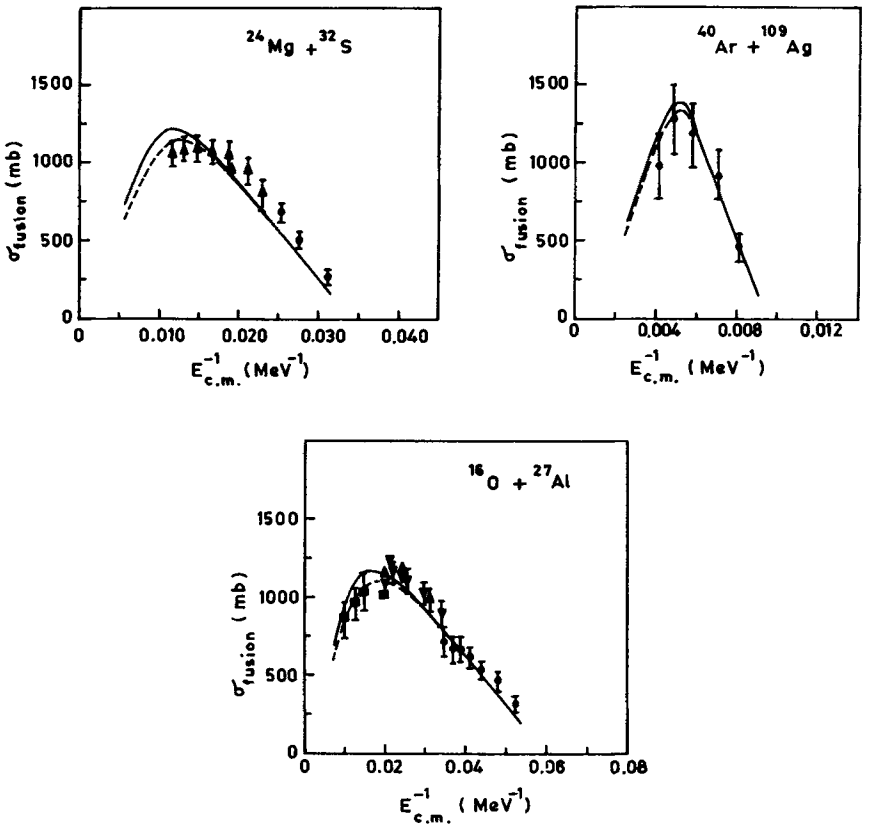

Figure 5. Fusion cross-section σ_{fus} plotted versus E_{cm}^{-1}. The solid line indicates our form of the potential, while the dashed line denotes the Bondorf potential. Data for different target projectile pairs are taken from various references detailed in the text.

Table 1. Barrier radius $R_B(l=0)$, barrier height $V_B(R_B, l=0)$, energy E^M_{cm} and cross-section σ^M_{fus} for the excitation maximum are tabulated. $l_f(\sigma^M_{fus})$ gives the angular momentum at the maximum of the excitation function.

Reaction	$R_B(l=0)$ fm	$V_B(R_B, l=0)$ MeV	$E^M_{cm}(\sigma^M_{fus})$ MeV	σ^M_{fus} mb	$l_f(\sigma^M_{fus})$
$^{16}O + ^{16}O$	7·67/7·76	10·86/10·77	42·5/36·4	1071/1060	23·50
$^{16}O + ^{24}Mg$	7·97/8·06	15·87/15·62	60·0/62·5	1138/1110	30·40
$^{16}O + ^{28}Si$	8·46/8·19	18·18/17·96	63·6/58·8	1165/1130	33·90
$^{16}O + ^{27}Al$	7·89/8·19	16·60/16·68	59·7/54·8	1180/1150	32·80
$^{24}Mg + ^{32}S$	8·52/8·62	29·40/29·40	88·6/85·1	1223/1170	47·50
$^{12}C + ^{27}Al$	7·95/8·01	12·70/12·76	47·8/46·5	1142/1120	26·30
$^{16}O + ^{40}Ca$	8·59/8·54	24·63/24·72	75·0/71·4	1227/1190	40·0
$^{35}Cl + ^{56}Fe$	9·35/9·64	60·60/60·99	142·0/135·1	1347/1260	79·0
$^{40}Ar + ^{109}Ag$	10·17/10·8	104·1/104·8	183·0/181·2	1376/1320	106·0
$^{35}Cl + ^{62}Ni$	10·17/9·79	64·6/64·77	150·0/138·9	1372/1290	83·8

First number – Author; Second number – Bondorf

5. Deformation vis-a-vis our model

The Coulomb self-energy of a spherical distribution of charge Ze, is given by $(3/5)(\mathbf{Ze})^2/R_0$, where $R_0 = r_0 A^{1/3}$. In the present formalism, there would be a decrease in the Coulomb self energy, depending upon the degree of overlap. This would lead to the self Coulomb energy,

$$E_c = (3/5)\frac{Z_{\text{eff}}^2 e^2}{R_{\text{eff}}}. \tag{9}$$

Further under the assumption of unaltered charge density, for each of the colliding systems, we can obtain an effective sphere of radius R_{eff}, containing the charge Z_{eff}, so that

$$Z/Z_{\text{eff}} = (R^3/R_{\text{eff}}^3) \tag{10}$$

when

$$R_{\text{eff}} = R(Z_{\text{eff}}/Z)^{1/3} = R(1 - K(\Omega)\Omega/V)^{1/3}. \tag{11}$$

From (9) and (11), Coulomb self-energy would be

$$(3/5)\frac{Z^2 e^2}{R}\left(1 - K(\Omega)\frac{\Omega}{V}\right)^{5/3},$$

for both projectile and target. In the region of small overlaps (i.e. $K(\Omega)(\Omega/V)$ is small) we can retain the first few terms of the series and get

$$E_c = E_{co}\left[1 - \frac{5}{3}K(\Omega)\frac{\Omega}{V} + \frac{5}{9}\left(K(\Omega)\frac{\Omega}{V}\right)^2 + \frac{5}{81}\left(K(\Omega)\frac{\Omega}{V}\right)^3\right] \tag{12}$$

where E_{co} is the Coulomb self-energy of either of the two spherical partners of full charge i.e. outside the overlap zone. The above form has a close identity with the LDM self energy (Vandenbosch and Huizenga 1973) for a distorted sphere (deformation α_2),

$$E_c = E_{co}[1 - \tfrac{1}{5}\alpha_2^2 - \tfrac{10}{49}\alpha_3^2 + \text{higher order terms}]. \tag{13}$$

Thus in this formalism we can simulate the situation with an effective deformation of the ions. Combining (12) and (13), we have a relation of the form

$$\frac{5}{3}K(\Omega)\left(\frac{\Omega}{V}\right) - \frac{5}{9}\left(K(\Omega)\frac{\Omega}{V}\right)^2 - \frac{5}{81}\left(K(\Omega)\frac{\Omega}{V}\right)^3 = \tfrac{1}{5}\alpha_2^2 + \tfrac{10}{49}\alpha_3^2 + \text{h.o. terms}. \tag{14}$$

Therefore one could, in principle estimate the amount of effective deformation which will be a function of the overlap volume. Here we have neglected the contribution of α_3 and other higher order terms. But one must remember, that depending upon the α_3 contribution for the same degree of overlap, the α_2 values will be lesser than what we get completely ignoring the higher order terms. The α_2 values have been computed for different degrees of overlap of various systems and are shown in table 2. Since at very large overlaps the flow pattern of the nucleons in the overlap zone will become

Table 2. $|\alpha_2|$ values for both heavy and light partners for various systems at different distances of separation and degree of overlap. The sign of α_2 is not determined.

Symmetric systems	D (fm)	Ω/V_L (%)	$\lvert\alpha_2\rvert$ (Heavy/Light)	Asymmetric systems	D (fm)	Ω/V_L (%)	$\lvert\alpha_2\rvert$ Heavy	$\lvert\alpha_2\rvert$ Light
	4·3	5·0	0·477		5·5	5·5	0·345	0·487
	3·9	9·6	0·656		5·1	10·0	0·464	0·654
	3·5	15·4	0·828		4·7	15·8	0·580	0·815
$^{12}C + ^{12}C$	3·2	20·5	0·952	$^{32}S + ^{16}O$	4·4	20·8	0·665	0·932
	2·9	26·2	1·07		4·2	24·5	0·720	1·00
	2·7	30·2	1·15		3·9	30·4	0·802	1·11
	8·2	5·1	0·482		9·1	5·4	0·371	0·486
	7·4	9·9	0·669		8·4	10·0	0·502	0·657
	6·7	15·3	0·826		7·8	14·8	0·611	0·798
$^{84}Kr + ^{84}Kr$	6·1	20·6	0·956	$^{138}Ba + ^{80}Se$	7·2	20·6	0·718	0·935
	5·6	25·6	1·06		6·8	24·8	0·787	1·02
	5·2	29·8	1·14		6·3	30·5	0·873	1·13
	11·1	5·1	0·480		9·8	5·0	0·232	0·439
	10·0	10·0	0·670		9·1	10·4	0·333	0·627
	9·1	15·1	0·819		8·6	15·3	0·403	0·756
$^{208}Pb + ^{208}Pb$	8·3	20·3	0·948	$^{208}Pb + ^{58}Ni$	8·2	19·7	0·458	0·857
	7·6	25·4	1·05		7·8	24·6	0·511	0·954
	7·0	30·1	1·14		7·4	29·9	0·563	1·04

more complex necessitating consideration of higher order terms of deformation in addition to the pure stretching ones (α_2), in table 2 we have restricted ourselves only to smaller overlap regions ($\Omega/V_L < 30\%$). Thus the α_2-values listed in table 2 are the maximal possible values of stretching deformations at the particular overlap originating from the neglect of α_3 and higher order deformation. Similarly on account of these dynamical deformations the ions will lose their surface definitions leading to corrections in their surface energies. Both these corrections viz. Coulomb and surface terms will naturally lead to a mass correction term in any potential energy calculation for a composite system. In analogy with the standard LDM deformation energy expression, here the deformation energy of each of the nuclei can be expressed (Vandenbosch and Huizenga 1973) as a function of the overlap volume.

We define the deformation energy as

$$\begin{aligned}\Delta E &= E^{\text{distorted}} - E^{\text{sphere}} \\ &= (E_s - E_{so}) + (E_c - E_{co}) \\ &= \left[\frac{5}{3}K(\Omega)\frac{\Omega}{V} - \frac{5}{9}\left(K(\Omega)\frac{\Omega}{V}\right)^2 - \frac{5}{81}\left(K(\Omega)\frac{\Omega}{V}\right)^3\right]\cdot(2E_{so} - E_{co}) \qquad (15)\end{aligned}$$

E_c and E_s stand for Coulomb and surface energies.

5. Conclusions

Thus one single form describes the Coulomb potential, from very large overlap (small separation distances $D \ll R_H + R_L$) to no overlap regions ($D \geqslant R_H + R_L$). Secondly,

the formalism opens up the possibility for visualizing the dynamical development of deformation degree of freedom, as a function of overlap volume, and hence with respect to the distance of separation of the two colliding nuclei. Such experimental data being not available quantitative agreement could not be checked. Our potential, at extremely small values of D builds up faster than the Bondorf potential. At degrees of overlap, where the lighter partner is almost sucked in (Birkelund *et al* 1979), the two body description of the Coulomb potential may not be very meaningful.

This parametrization of the Coulomb potential has special significance not so much for the fusion calculations as such, since the fusion cross-sections are not significantly different from that of Bondorf. But its significance is obvious if we consider the evolution of the shape from a dinucleus (separated colliding ions) to a uninucleus (fused state). At smaller overlaps, a small neck is formed, the neck matter content being 2Ω. At larger overlap the neck matter will swell and due to flow out at constant density in transverse direction, will fill up the wedge volume between the two spherical entities and form a smooth transverse bulge giving a fused uninucleus at a deformed or spherical state. This is in conformity with the two centre parametrizations used in fission and fusion (Maruhn and Greiner 1972; Fink *et al* 1974). Secondly the potential opens up the possibility of visualizing the evolution of deformation of the colliding heavy ions with the degree of overlap. At large distances $D \geqslant R_H + R_L$, where there is no overlap the individual ions are spherical or nominally deformed. But with the increase of overlap in the region $D < R_H + R_L$, the individual surfaces of the ions are more and more smeared as the overlap grows signifying build up of deformation to a particular extent, where a single deformed uninucleus surface evolves.

Such visualization of the shape evolution (evolution of collective degrees under flow of matter) is not obvious from the Bondorf potential. Thus the present model, though has a somewhat complex parametrization, preserves all the merits of Bondorf potential so far as fusion cross-sections and matching at $D = R_H + R_L$ are concerned and in addition helps visualization of the fusion path in terms of the evolution of shape from a separated dinucleus to a fused uninucleus.

Acknowledgement

The discussions with Drs S Samaddar, R K Moitra, D Bandhopadhyay (SINP) and Dr J N De (BARC) are acknowledged with thanks.

References

Back B, Betts R R, Gaarde C, Larsen J S, Michelsen E and Kuang-Hsi Tai 1977 *Nucl. Phys.* **A285** 317

Banerjee A K, Samanta B C and Samaddar S K 1985 *Phys. Lett.* **B153** 213

Birkelund J R, Tubbs L E, Huizenga J R, De J N and Sperber D 1979 *Phys. Rep.* **56** 107

Blocki J, Randrup J, Swiatecki W J and Tsang C F 1977 *Ann. Phys. (NY)* **105** 427

Bohr A and Mottelson B R 1975 *Nuclear structure* (Massachusetts: Benjamin, Reading) Vol. II

Bondorf J P, Sobel M I and Sperber D 1974 *Phys. Rep.* **15** 83

Britt H C, Erkkila B H, Stokes R G, Gutbrod H H, Plasil F, Ferguson R L and Blann M 1976 *Phys. Rev.* **C13** 1483

Brogila R A and Winther A 1981 *Heavy ion reactions* (New York: Benjamin/Cummings) **1** 46

Conjeaud M, Harar S, St. Laurent F, Loiseaux J M, Menet J and Viano J B 1977 *Proc. Symp. on macroscopic features of heavy-ion and pre-equilibrium processes* Hakone, Japan (quote in Bonche P, Grammaticos B and Koonin S 1976 *Phys. Rev.* **C17** 1700)

Dauk J, Lieb K P and Kleinfeld A M 1975 *Nucl. Phys.* **A241** 170
Eisen Y, Tserruya I, Eyal Y, Fraenkel Z and Hillman M 1977 *Nucl. Phys.* **A291** 459
Fernandez B, Gaarde C, Larsen J S, Pontoppidan S and Vidabaek F 1978 *Nucl. Phys.* **A306** 259
Fink H J, Maruhn J, Scheid W and Greiner W 1974 *Z. Phys.* **268** 231
Gutbrod H H, Winn N G and Blann M 1973 *Nucl. Phys.* **A213** 267
Hodgson P E 1978 *Nuclear heavy-ion reactions* (Oxford: University Press)
Jain A K, Gupta M C and Shastry C S 1975 *Phys. Rev.* **C12** 801
Kolata J J, Fuller R C, Freeman R M, Hass F, Heusch B and Gallman A 1977 *Phys. Rev.* **C16** 891
Kovar D G, Bond P D, Flaum C, Levine M J and Thorn C E 1977 *Bull. Am. Phys. Soc.* **22** 1019
Kozub R L, Lu N H, Miller J M, Logan D, Debiak T W and Kowalski L 1975 *Phys. Rev.* **C11** 1497
Maruhn J and Greiner W 1972 *Z. Phys.* **251** 431
Park J Y, Scheid W and Griener W 1981 *Dynamics of heavy-ion collisions (Proc. of 3rd adriatic europhysics Conf. Hoar. Croatia,* Yugoslavia (eds) N Cindro, R Ricci and W Greiner (Amsterdam: North-Holland) p. 53, May 25–30
Randrup J 1978 *Ann. Phys. (NY)* **112** 356
Rascher R, Muller W F J and Lieb K P 1979 *Phys. Rev.* **C20** 1028
Scheid W, Ligensa R and Greiner W 1968 *Phys. Rev. Lett.* **21** 1479
Scobel W, Gutbrod H H, Blann M and Mignerey A 1976 *Phys. Rev.* **C14** 1808
Spinka H and Winkler H 1974 *Nucl. Phys.* **A233** 456
Tabor S L, Geesman D F, Henning W, Kovar D G, Rehm K E and Prosser F W 1978 *Phys. Rev.* **C17** 2136
Tserruya I, Eisen Y, Pelte D, Gavron A, Oeschler H, Berndt D and Harney H L 1978 *Phys. Rev.* **C18** 1688
Weidinger A, Busch F, Gaul G, Trautmann W and Zipper W 1976 *Nucl. Phys.* **A263** 511
Wilczynski J and Siwek-Wilczynska K 1975 *Phys. Lett.* **B55** 270